Marine Pollution Bulletin 161 (2020) 111723

Contents lists available at ScienceDirect

Marine Pollution Bulletin

journal homepage: www.elsevier.com/locate/marpolbul

Three-dimensional numerical modelling of transport, fate and distribution of microplastics in the northwestern Arabian/Persian Gulf

Y. Alosairi, S.M. Al-Salem*, A. Al Ragum

Environment & Life Sciences Research Centre, Kuwait Institute for Scientific Research (KISR), P.O. Box 24885, Safat 13109, Kuwait

ARTICLE INFO

Keywords:
Microplastic
Lagrangian particle tracking
Model
Gulf
Plastic waste

ABSTRACT

Marine plastic litter has been a major concern over the past decade particularly in semi-enclosed seas such as the Arabian/Persian Gulf, which are likely to impose a relatively higher threat to ecosystem and human health. In this work, we have focused our efforts on the transport features of marine surface microplastics (MPs) in the Gulf. The assessment utilizes a 3D hydrodynamic model of the northern Gulf which was coupled with a particle tracking model. We have considered five release locations and investigated two dominant wind conditions by applying different numerical scenarios. The results revealed that the northerly winds result in high dispersion and seaward transport of MPs in the open coastal zones, while in semi-enclosed regions they result in high trapping and beaching verified by visual investigation. The study shows that further detailed field investigations are warranted to enable the models to better parameterize the fate and distributions of MPs.

1. Introduction

Our current times have been termed the 'Plastics Age' due to our ever-increasing dependency on polymeric products and commodities for more than 50 years (Al-Salem et al., 2018a, 2018b; Ryan, 2015). Plastics provide a hygienic surface for packaging, and are durable, light weight and versatile by their nature. This results in ever-increasing solid plastic waste generation rates around the globe, estimated at 274 million tonnes annually (Geyer et al., 2017). Some 12.7 million tonnes of plastic debris are categorised as a major component of marine litter after entering the world's oceans and water bodies (Jambeck et al., 2015). This fraction of the debris is associated with mismanaged plastic solid waste that accumulates in and around marine areas. Social behaviour and lack of infrastructure in the countries contributing extensively to this type of waste are the main reasons for this waste accumulation.

Concern is now rising about microscopic marine litter, triggering research into its association with the health of seafood consumers and marine environments (Andrady, 2011, 2017; Hidalgo-Ruz et al., 2012; Kor and Mehdinia, 2020; Hahladakis and Aljabri, 2019; Lyons et al., 2020). Moreover, attention is being paid to the impact of plastics on marine species because the majority of plastic articles that fragment and become marine litter contain persistent pollutants and toxins from the additives and plasticizers used in their manufacture (Ouyang et al., 2020). In particular, microplastics (MPs) have been an extremely important topic in research and academic circles. This has covered:

- the ease with which MPs are mistaken for prey by a variety of marine species (Al-Salem et al., 2020a)
- the impact on the marine environment as a persisting pollutant (Andrady, 2017; Burns and Boxall, 2018; Al-Salem et al., 2020b; Tang et al., 2020)
- adsorption of various harmful hydrophobic pollutants acting as pollutant transport vectors (Wagner et al., 2014)
- transfer of pollutants into the food chain (Oliveira and Almeida, 2019) and
- passive uptake by fish from gear and nets through gill water filtration (Barboza et al., 2019).

MPs are defined specifically as particles of size ≤ 5 mm, the term first used in 2004 to describe plastic litter of microscopic size (Thompson et al., 2004). Confusion can occur between the terms 'microplastics' and 'microlitter', the latter defined as debris that can pass through a 500 μm sieve and possesses a diameter between 0.06 and 0.5 mm (Gregory and Andrady, 2003).

Recent MPs research has focused on its quantification and distribution, from early reports on coastlines in the early seventies (Carpenter and Smith Jr., 1972) to deep-sea oceans (Oliveira and Almeida, 2019) have received attention. Gut contents of marine species have been used as MP indicators in various water bodies including the

* Corresponding author.
E-mail address: ssalem@kisr.edu.kw (S.M. Al-Salem).

https://doi.org/10.1016/j.marpolbul.2020.111723
Received 18 August 2020; Received in revised form 24 September 2020; Accepted 24 September 2020
Available online 07 October 2020
0025-326X/ © 2020 Elsevier Ltd. All rights reserved.

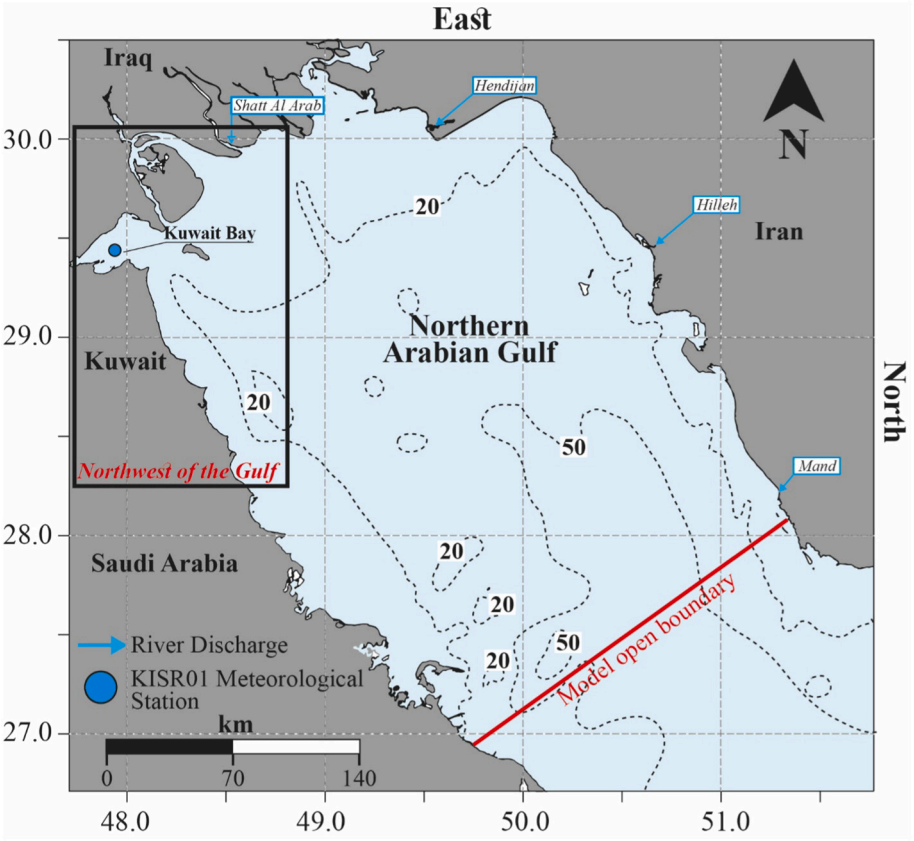

Fig. 1. The Geophysical Characteristics of the Northern Gulf Including the Area Of The Study, Numerical Model Open Boundary, and KISR01 Meteorological Station. Note to reader: Image courtesy of Kuwait Institute for Scientific Research (KISR) – Met Station.

North Sea, the Mediterranean Sea, and Atlantic and Pacific Oceans (Law et al., 2010; Bergmann et al., 2015; van der Hal et al., 2017; Clukey et al., 2017). On the other hand, research along the Arabian Gulf (also known as the Persian Gulf or the Gulf of the Inner Sea of the Regional Organization for Protection of the Marine Environment, ROPME) (Hamza and Munawar, 2009), is very scant (Fig. 1). From this point onwards, this marine body will be referred to as 'the Gulf' in this manuscript: more details on its main characteristics will be detailed in the next section. Recently, a few studies have emerged from Iran quantifying MPs along a limited number of coastlines and estuaries. Most results showed that MPs comprised polyethylene (PE), polypropylene (PP) and polystyrene (PS) resins, reaching hundreds in a particular location along the Iranian coastline in the form of microscopic fibres or pellets (Abbasi et al., 2018; Akhbarizadeh et al., 2017; Aliabad et al., 2019; Naji et al., 2017a, 2017b, 2018, 2019). Al-Salem et al. (2020a) recently detected MP particles ranging from 0.96 to 1.57 mm in the gut of fish-stocks of commercial importance along the Kuwaiti coastline, namely *Acanthopagrus latus*, *Eleutheronemaa tetradactylum* and *Lutjanus quinquelineatus*. From the nature of this type of fish, found in muddy waters and sheltered lagoons habitats, the MPs were suspected to arise from primary sources (i.e. waste fragmentation). Abayomi et al. (2017) surveyed eighty beaches in Qatar and studied sediment and seawater samples, reporting 1 to 5 mm fibres with an abundance on the surface of 4×10^4 to 10^6 particles km^{-2}.

Given the interconnected mechanical, chemical, and biological processes that influence distribution and transport of marine plastic litter, understanding the detailed processes is paramount. The complexity arises from the heterogeneity in the form of plastic particles which varies considerably depending on the degrading conditions. As a result, the particles behave in a non-linear way throughout the water column (Mahdavimanesh et al., 2013). The disparity in the MP particle behaviour is associated with varying density, buoyancy, and residence times which change throughout their life cycle in the water (Dong et al., 2018). Therefore, answering the question of how plastics are being transported in marine systems and where it accumulates is more challenging if the full lifetime is considered, because the time scale can extend to many years, depending on the type and degradation history of the polymeric resin (Al-Salem, 2019a). Currently, research is continuing to further understand this behaviour since understanding these processes enables the evaluation of the ecological impacts and the assessment of the human health risks. Also, it aids in formulating policy and guidelines for coastal management and for implementation of suitable monitoring programs (Rangel-Buitrago et al., 2019).

Numerical models are promising tools for gaining better insights into the behaviour of plastics once they have entered dynamic flow systems (Hardesty et al., 2017). Many of the complexities associated with flow processes can be computed by numerical models. In addition, advances in computational capacity and numerical techniques have enabled the implementation of fine grid resolution to compute detailed and accurate flow patterns which act as drivers for MPs. Numerical hydrodynamic computations are typically coupled with either Eulerian or Lagrangian pollutant models. The Lagrangian trajectory model employs a moving frame of reference, while the Eulerian grid model uses a fixed coordinate system with respect to space (van Utenhove, 2019). The choice of approach depends on the spatial and temporal nature of the problem that needs to be resolved. As an example, Alosairi and Alsulaiman (2020) utilized a Eulerian approach for the dynamics of the dissolved oxygen in Kuwait Bay, hereafter refer to as 'the Bay'. A similar approach was followed in the Alosairi et al. (2011) study for the mixing and dispersion processes in the Gulf waters. In contrast, Lagrangian particle tracking models are frequently utilized to study the transport and fate of plastic particles in oceans (van Utenhove, 2019; Collins and Hermes, 2019; Isobe et al., 2014) because of the advantage of resolving particle displacements at sub-grid scales while maintaining a

reasonable computational cost. Núñez et al. (2019) studied the probabilities of marine litter accumulations in Santona Bay (Spain) by utilizing a combination of statistical analysis and numerical models based on Lagrangian methods. The particle tracking model provided vital details about the potential trajectories of the litter. Politikos et al. (2020) utilized Lagrangian particle tracking coupled with hydrodynamic model to assess the transport, residence time and connectivity of floating litter in the Eastern Ionian Sea. The study relied on particle count to estimate the percentage of litter that was washed offshore and that which was retained within the coastal waters. A similar model was implemented by van Utenhove (2019) to assess the horizontal dispersion and transport of macroplastics under various numerical settings and to quantify and determine their fate.

Within the Northern Gulf context several studies have been conducted to understand the hydrodynamic processes. Alosairi and Pokavanich (2017) studied the seasonal variations around Kuwait Bay using a layer integrated approach. The study revealed variations of the residual flow velocity in 3D and considered the meteorological, tidal, and density gradients effects. Alosairi et al. (2011) studied hydrodynamic processes and assessed various aspects of the dynamic regime in the Gulf including wind induced flows, formation of multiple scale gyres, and mixing and dispersion. The literature surveyed for the Gulf has also formed a good basis to study the transport and fate processes of waste plastics (Pous et al., 2012, 2013a, 2013b; Kämpf and Sadrinasab, 2006; Thoppil and Hogan, 2010). This is due to the fact that well-validated hydrodynamic models have been used previously to act as the driver for either dissolved or particulate pollutants, providing a detailed understanding of these processes in the Gulf.

In the current study we identify the hydraulic processes at intermediate fields (i.e. 1 to 50 km) which correspond to the most diverse water current conditions controlling MPs transport in the NW Gulf (Fig. 1). These fields control the transport, fate and horizontal distributions of MPs which are released from Kuwait's coastline, indicated by the black box in Fig. 1. The MPs source investigated was anthropogenic primary plastics contributing to municipal solid waste and marine litter. For the summer conditions the assessment utilizes a 3D hydrodynamic model previously validated for the Northern Gulf area (Alosairi and Pokavanich, 2017). The hydrodynamic model is coupled on an offline basis to a particle tracking model. Using this coupling technique several numerical Scenarios were implemented to estimate the effects of dominant winds on the surface transport and distribution for MPs. An additional Scenario has been considered to assess the transport effects of reverse estuarine circulations found in the Bay area and the supply processes to the NW Gulf.

The work presented in this study addresses a major gap in the literature because the transport and fate of marine litter MPs are addressed in only a few studies (Mahdavimanesh et al., 2013; Stuparu et al., 2015; Núñez et al., 2019; Palatinus et al., 2019; Rangel-Buitrago et al., 2019). The numerical results were also discussed in light of findings of fish stock populations around the Bay area (in particular) and the Gulf (in general). This approach can help decision-makers and decision-takers in developing strategies that may be the first of their kind for the control of marine litter and MPs distribution around the Gulf.

2. Methods

2.1. Study area

The area under consideration is the NW part of the Gulf specifically along Kuwait coastline (*Long. 47 and 49°E*; *Lat. 28 and 30°N*). Fig. S1 of the Supplementary material file depicts the Gulf in relation to neighbouring countries and the Gulf of Oman. The Gulf in general is considered to be a weak estuary due to the limited inflow of freshwater compared to its geographical scale. However, it is worth noting that the NW is influenced by Shatt Al-Arab River (see Fig. 1), providing diversity to marine species for which it is a natural habitat (Al-Husaini et al., 2015). The length of the Gulf is almost 1000 km and its width is approximately 330 km (Fig. 1). On the other hand, the NW part of the Gulf is relatively narrow compared to southern areas, with a width of 218 km between Kuwait and Saudi Arabia at the western side and Iran at the eastern side. The mean depth of the Gulf is 36 m with deeper waters (> 50 m) in the east closer to Iranian coastline. The topographical nature of the northern Gulf means that tides account for most of the currents throughout the water column, particularly near the shallow western coast (Alosairi and Pokavanich, 2017). Tides in the NW are generally described as mixed semidiurnal (Alosairi et al., 2018a, 2018b). Due to the hydrographical setting of the basin, a relatively larger diurnal component of tides is found in the NW compared to the semidiurnal. The semidiurnal tides develop into two anticlockwise amphidromic systems, one located in the northern Gulf. These characteristics cause the NW Gulf to exhibit a dynamic behaviour that is subject to interplaying forces including winds, river discharge and tides. More details about the main characteristics of the Gulf may be found elsewhere (Al-Sarawi et al., 2018; Alosairi et al., 2018b; Al-Salem et al., 2020b; Lyons et al., 2020). Kuwait Bay, located in the NW Gulf, is relatively shallow water with a mean depth of 6 m (Fig. 1). The Bay experiences mixed semidiurnal tides with a comparatively higher tidal range that reaches 4.6 m. The main channel of the Bay is relatively deep, exceeding 15 m in some areas. The northern and southern areas of the Bay are fringed with large tidal flats, considered sources of saline waters due to extreme evaporation during the summer. Collectively, these hydrographical characteristics result in reverse estuarine circulations at the main axis (Alosairi et al., 2018b).In regions such as Shatt Al-Arab, the estuarine fields are limited due to the strong current that plays a large role in horizontal dispersion. Such processes of a mechanical nature do not allow large effects to reach the Bay of the southern coast. In addition, the Bay western areas are shallow with high evaporation and discharge of brine waste that enables the water to sink due to possessing high density, and therefore the residual flow is reversed (Alosairi et al., 2018a; Al-Salem et al., 2018b). The current study also addresses the transport of MPs associated with the reverse estuarine circulations in the Bay.

2.2. Description and configuration of hydrodynamics model

The numerical model (Delft3D) was utilized in this study. The model was originally developed by Deltares Delft Hydraulics which is a comprehensive and well-established numerical modelling environment encompassing several modules that enables the study of hydrodynamics, water quality, sediment transport and particle tracking. The configuration of the model is applicable to coastal, river, lake and estuarine water bodies (Deltares, 2011; Alosairi and Pokavanich, 2017; Alosairi et al., 2018b; Herdman et al., 2018; Oliveira et al., 2019; Erdik et al., 2019). The detailed description and configurations utilized for the hydrodynamics and the particle tracking, respectively, are given below.

The hydrodynamic module Delft3D-FLOW is utilized in the current study. It solves the depth-averaged (2D) or layer-integrated (3D) non-linear shallow water equations, which are derived from the Navier-Stokes fluid-dynamic equations for incompressible free surface flow. The model utilizes a curvilinear grid while a flexible grid version is also possible (Deltares, 2011). These equations provide hydrodynamic modelling with a detailed mathematical solution for time-dependent tidal force, varying wind fields, and density gradients associated with temperature and salinity. For the current study, a 3D configuration was adopted in which the shallow water equations are simplified so they can be integrated over the thickness of each layer in the vertical direction for effective computation (Alosairi and Pokavanich, 2017). These settings reduce the spatial domain into 3D containing ten varying layer thickness that represent the depth under the hydrostatic assumption. Given the objectives of the study, higher vertical resolutions were

Table 1
General numerical settings utilized in the hydrodynamic model.

Water density (kg/m^3)	Wind drag (at 25 m s^{-1})	Horizontal viscosity (m^2 s^{-1})	Horizontal diffusivity (m^2 s^{-1})	Secchi depth (m)	Dalton number
1028	0.0027	5	10	4	0.0006[a]

Note to reader.
[a] Dimensionless.

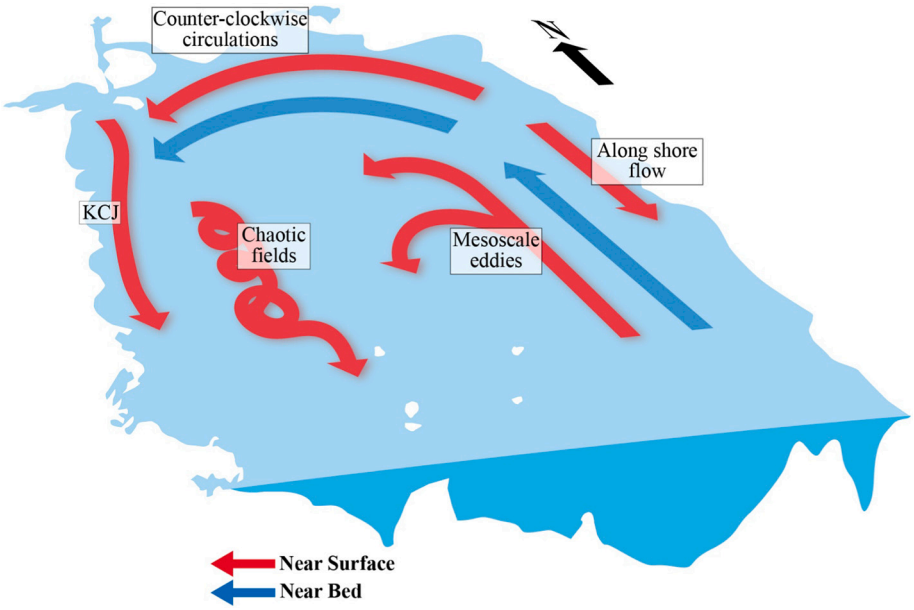

Fig. 2. Three-dimensional residual circulation patterns of the Northern Gulf during the summer season, reconstructed from Alosairi and Pokavanich (2017).

imposed near the surface as it is assumed that the MPs remain in the upper layers. Given the relatively small aspect ratio of the Northern Arabian Gulf area where the horizontal length scale of several kilometres is much larger than the vertical scale (several meters), the shallow water assumptions are valid.

Since the hydrodynamic model given by Alosairi and Pokavanich (2017) acts as the driver for the particle tracking model, it is worth addressing the main numerical settings. These are shown in Table 1 along with general the circulation patterns (Fig. 2). Short temporal scales (e.g. 3 to 15 days) were our focus in this study. Therefore, the summer circulations, specifically July, serve well for this purpose as this seasonal period is considered to be the harshest in the Gulf (Alosairi et al., 2018b). It is worth noting that for the settings of the current study, the horizontal grid resolutions of the model were refined to 800 × 800 m at the coastline of the studied region. This refinement was implemented to best serve the particle tracking model from numerical perspectives. The forcing of the hydrodynamic model at the open boundary and rivers remained the same as Alosairi and Pokavanich, (2017) in terms of temperature and salinity (see the model boundary locations in Fig. 1). However, the meteorological effects were updated with recent data for the summer of 2018 obtained from station KISR01 in the Bay (Fig. 1). The water levels at the open boundary for the summer of 2018 were derived from tidal constituents in a similar fashion to that of Alosairi and Pokavanich (2017).

2.3. Circulations of the Northern Gulf

The key circulation features addressed previously by Alosairi and Pokavanich (2017) were computed using detailed model-forcing and were validated for the temporal and spatial variations of temperature, salinity and density. The study suggested that during summer the climatic effects establish a clear baroclinic setting throughout the Northern Gulf. The heat exchange is clearly largest during summer and therefore the thermocline is well defined in the deep regions of the basin. The strong north-westerly winds are associated with high air temperatures frequently exceeding 50 °C and providing strong surface circulation due to the vertical density gradient where thin warm layer overlay the cooler deep waters. As a result, a strong counter-clockwise circulation occurs at the northern edge of the basin (Fig. 2). On the Iranian side, which is comparatively deeper, weaker circulations prevail but with a clear vertical variation in the currents along the coast. Seaward flow is found along the coast near the surface, a landward flow near the bed. These features are generally associated with the weak Indian Ocean Surface Water which advances via the Strait of Hormuz and along the deeper Iranian coast (Fig. 2). Most relevant to the current study is the NW Gulf where MPs are likely to be released. Stronger along-shore currents, known as the Kuwait Coastal Jet (KCJ), dominate the western shoreline (Fig. 2). Due to the topography, the strong currents are generally induced by tides, which are highest at the NW corner of the basin. The effects were enhanced by the actions of episodic warm winds (Shamal) which aid the transport southwards during summer. Another key feature found near the western coast in the surface water is a strip of non-uniform flow named 'Chaotic Fields' (Fig. 2). The authors suggest that such circulations are formed due to the imbalance in buoyant regimes in that location. Along the central axis, several mesoscale eddies are exhibited towards the SE. The cyclonic features at the central axis are highly controlled by the wind regime (Pous et al., 2013a, 2013b). It is worth noting that Alosairi and Pokavanich (2017) concluded that the surface current, which would largely control the transport processes, are more pronounced during summer than other seasons, particularly along the shore.

2.4. Description of particle tracking model

To simulate the transport and fate of MPs by the means of particle tracking, Delft3D-PART has been utilized (Delft3D, 2018), using the

hydrodynamic information provided by Delft3D-FLOW to track particles in 3D over a given time. In addition, the dynamic concentration distribution was available by computing the mass of particles in the model grid cells. The processes in Delft3D-PART are assumed to be deterministic except for the random displacement of particles at each time step. The particle tracking adopted in Delft3D-PART is based on random-walk since the simulated behaviour is stochastic and the number of particles is limited (Rubinstein, 1981). Spatially, Delft3D-PART allows for detailed description by resolving the sub-grid concentrations of a given substances. Given these numerical bases, Delft3D-PART is best suited for mid-field transport and dispersion within the range of 1 to 50 km which is the situation for our case. The key physical processes considered in the model are advection and diffusion. Advection represents the transport of MPs by water flow and wind drag, while diffusion is described by random displacement. Resolving these processes within Delft3D-PART has two steps: firstly, the transport by advection on the basis of shear stresses, and secondly the diffusive displacement of particles. The advection is given by the local current velocity fields which are computed by Delft3D-FLOW, and additional advection due to windage (wind-induced drift of the floating particles) can be prescribed. The velocity of the particles is given as the vectoral sum of local current and the windage effects, thus:

$$V_{adv} = V_{local} + V_{wind} \quad (1)$$

where V_{adv} is the velocity of the particle, V_{local} is the local velocity and V_{wind} is the velocity due to windage. As for the unresolved sub-grid dispersion, it is evaluated by the means of random walk as represented below

$$dX'(t) = R_x\sqrt{2D\Delta t} \quad (2)$$

$$dY'(t) = R_Y\sqrt{2D\Delta t} \quad (3)$$

where R represents a random number generated at each time step in Delft3D-PART. The value of R ranges from -1 to $+1$ and has uniformly distributed statistical properties with a mean of zero, D represents the diffusivity while Δt represents the Lagrangian time step (Delft3D, 2018). For this numerical approximation, the diffusion coefficient accounts for all the random fluctuations caused by small scale deviations in the flow fields and the winds that occur at sub-grid scales. The distance of the random displacement is a function of the sub-grid diffusivity and the set time step in Delft3D-PART. The diffusion coefficient is assumed to be isotropic, but the corresponding random displacements are computed for x and y directions separately (Delft3D, 2018). The additional effect from wind-induced drift of floating particles can be imposed in Delft3D-PART, advection due to windage being given as follows (Delft3D, 2018):

$$V_{wind} = C_{wd} \times (V_w - V_{current}) \quad (4)$$

where C_{wd} is the wind drag coefficient, V_w is the wind speed at 10 m above the mean sea level and $V_{current}$ is the flow velocity. Since the drag coefficient is an empirical representation of object characteristics, the increase of the coefficient results in further advection of particles. For the beaching of particles, a probabilistic approach is used (Delft3D, 2018). Delft3D-PART utilizes a sticky probability with a model setting can vary between 0 and 1. The higher the value, the greater the number of particles that are beached once in contact with the coastline. Further details about the numerical representation of the processes are given in Delft3D (2018).

2.5. MPs release sites

To investigate the transport, fate and distribution of MPs in the NW Gulf, five sites have been selected along the Kuwaiti coastline as release points (Fig. 3). The location of each site is also given in Table 2 for convenience. The selection of the sites was based on three criteria:

- the anthropogenic human activities that contribute to the accumulation of plastic solid waste as a primary source of MPs along the coastline
- the population density of the residential governorate (of the State of Kuwait) that influences the extent of littering
- the prevailing dynamics at each site of the release which control the MPs behaviour.

Therefore, the release points are widely distributed along the coastline and generally in the vicinity of unique receiving dynamics (Fig. 3a), aimed at capturing the dominant fate and transport processes spatially and temporally.

The first release site is the northern location of Subiya (SB), characterized by shallow water, mudflats, and within the flow way of Khor Al-Subiya (Fig. 3b). Given the strong tidal regime that controls much of the flow, the release of the particles is within multi-directional streams towards the northwest at high tides and southeast during low tides. At high tide the flow contracts due to the narrow Khor Al-Subiya resulting in high momentum (Fig. 3b). At low tide the channel is flushed, resulting in turbulent fields. The current flows during the spring tides can reach as high as 1 m s^{-1} (Alosairi et al., 2015). Currently, the Subiya area is under urbanisation and major plans are made to deploy a new city at this location (Fig. 3a highlighted in yellow). Potentially, SB is a source of littering for plastic solid waste within construction and demolition activities. SB is also associated with recreational activities along the marine causeway located by the tip of Subiya headland which adds to the accumulation of waste and consequently its fragmentation and release into marine environment. On this basis, the location was selected in the current study.

Inside the Bay two release locations were considered, Jahra (JH) and Salmyia (SL) shown respectively in Fig. 3c and d. Each of these locations was chosen for a particular reason that makes it a potentially important release point for MPs along the coastline. First, the prevailing dynamics vary considerably across these locations. The JH site is within the Jahra Bay at the innermost region in Kuwait Bay (Fig. 3c). Due to its semi-enclosed nature and the large mud flat, low dynamics prevail compared to the rest of the Bay. Similar characteristics also apply to Sulaibikhat Bay but this bay is double the area of Jahra Bay and has slower flushing (Pokavanich and Alosairi, 2014). Both release sites are surrounded by relatively high populations, commercial sectors and industries associated with littering. Naji et al. (2017b) found that the sediments with the highest number of plastics are from sites in the vicinity of highly populated centres and municipal wastewater discharges in the Gulf. Furthermore, the JH site is near the second largest active landfill of Kuwait, with municipal solid waste including some 18% plastics (Al-Salem et al., 2018a, 2018b). There is no segregation within the activities of the landfill site and lack of a material recovery facility causes cross-contamination of plastics that could be released as debris to the Bay (Al-Salem, 2019b). Details of quantities of waste of which plastics are a major component and further details on estimated MPs in the Gulf can be found elsewhere (Al-Salem et al., 2020b). In addition, the JH site is associated with MPs release due to the argillaceous (clayey) nature of the sediment that acts as a trap. It is considered that the release at JH is representative of MPs within Jahra Bay.

For the SL release site, the hydrodynamics are more pronounced and characterized by strong turbulent fields. The strong dynamics are driven by the water-land interactions which create eddies, particularly at headlands (Fig. 3d). As these eddies are associated with the tides interacting with the headland, they are strong and large during spring tides and smaller ones during neap tides. The currents within these fields occasionally exceed 1 m s^{-1} near headlands. Turbulent dispersion defines the mixing processes in this area (Alosairi et al., 2011). Between the Salmiya and Bnaid Al-Gar headlands there is an alongshore current, with prominent flow in the seaward direction (Fig. 3d). The full length of the coastline in this region is highly populated including extensive commercial and recreational activities. The most

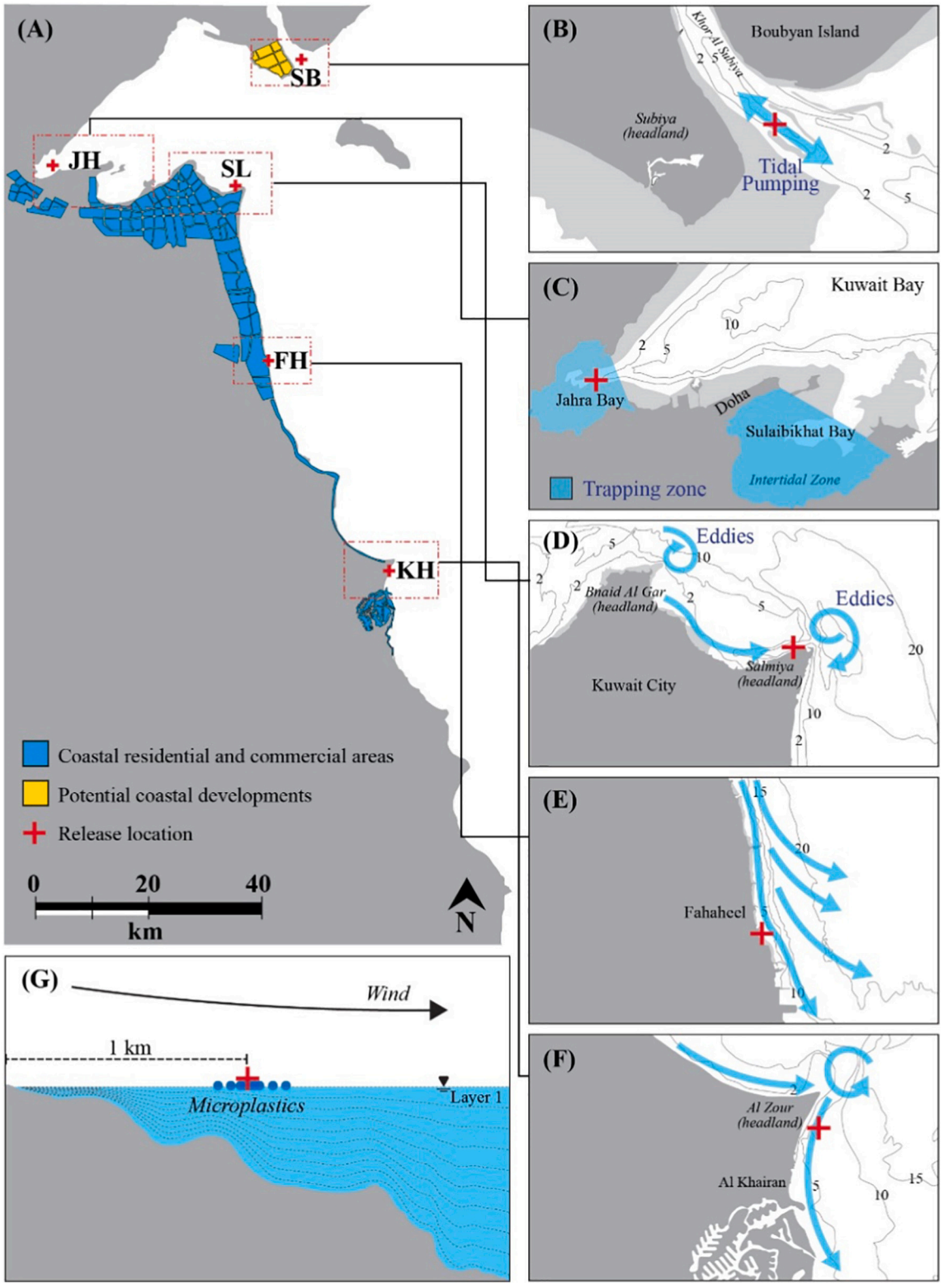

Fig. 3. Microplastics release locations at (a) the NW of the Gulf. The hydrographical characteristics at the individual locations in (b) mouth of Sabiya channel, (c) mouth of Jahra Bay, (d) Salmiya headland, (e) Fahaheel, (f) head land of Al Zour, (g) dominate the typical vertical configuration at the release locations.

representative is the selected location indicated in Fig. 3d.

At the southern coast of Kuwait two releases sites were chosen, Fahaheel (FH) and Khiran (KH), shown in Fig. 3e and f, respectively. Although the locations appear similar geographically, they experience different flow patterns (Fig. 3e and f). In the FH region, the cross-shore bathymetry markedly shifts from shallow (~5 m) near-shore to 15 m within just 1.7 km from the shore. This enables flow streamline divergence towards the southeast of the Gulf. The orientation of the flow is therefore well aligned with the dominant Shamal winds that should aid a seaward transport regime. In the KH area the cross-shore bathymetry is smoother in transitioning to the deep waters and the tidal current is less significant due to the smaller ranges. Therefore, the flow is mostly

Table 2
Details of the release locations of the particles depicted using the Universal Transverse Mercator (UTM) and mean depth in each site.

Location	Longitude	Latitude	Mean depth at release point (m)
Sibiya (SB)	227,354.2	3,272,867.5	5.3
Jahra Bay (JH)	182,010.9	3,252,486.3	5.2
Salmyia (SL)	214,761.4	3,250,843.0	10.0
Fahaheel (FH)	222,308.7	3,220,022.3	9.3
Khiran (KH)	245,047.2	3,176,195.3	5.1

directed towards the south and the streamlines are along the shore. Both locations are characterized by activities associated with marine littering. In FH commercial and recreational activities similar to SL exist from its over 100,000 residents and surrounding industries (Al-Qassimi and Al-Salem, 2020), but KH is dominated by industry and by beach houses which are used during summer.

It is important to note that the particular release position at each location varies from site to site. In the shallow areas which are associated with tidal mudflats, as in JH and SB, the release is relatively deep and offshore. This avoids an unrepresentative beaching of the particles that could occur during the initial simulation. Releases at SL, FH and KH are made near the shore but keeping a distance of 1 km from the shoreline in areas devoid of mudflats (see Fig. 3g), valid for the purpose of the study since we aim to assess the intermediate transport fields. At the shoreline more complex processes associated with wave interactions results in different distributions and offshore transport.

2.6. Numerical scenarios

To assess the effects of the various parameters forces on the transport and fate of MPs, several Scenarios were implemented and compared. Since we aim to provide an insight into the intermediate fate and transport time scales of MPs, we have focused on two dynamic conditions. The first is *dominant winds*, while the second is *reverse estuarine circulation* due to vertical density gradients, the former acting over relatively shorter periods than the latter. The northwesterly winds (Shamal) and the southeasterly winds (Kous) have been reported previously to dominate the meteorological regime of the NW Gulf (Fig. 4a). During summer the Shamal are more frequent than Kous and can last longer. The two wind regimes counteract in terms of directions, therefore the resulting transport and fate of MPs at the surface would vary accordingly. It is worth noting that the wind regime and the reverse estuarine circulations in the Bay are interactive, and therefore, results in varying dynamic regime. The Shamal results in weakening the reverse estuarine conditions. While for the low Kous winds, it has much less effects in disturbing the reverse estuarine fields and perhaps prolongs it during neap tide specifically.

Two numerical wind condition scenarios have been considered (Fig. 4a). Scenario 1 represents Shamal conditions, while Scenario 2 represents Kous. For the numerical settings of both Scenarios, all the locations have been considered, as in Table 2 including the numerical settings in Table 3. The only differences are the wind direction and speed which remained constant for each Scenario. For Scenario 1, the winds were set to blow from the NW (330°) and a speed of 3.4 m s^{-1}; Scenario 2 were SE (135°) and 2.6 m s^{-1}. It is worth noting that the winds in both Scenarios act evenly across the entire domain, speed and direction remaining constant throughout the simulation period. Although the wind varies in reality, this is a hypothetical condition to assess the transport mode of each wind settings.

In Scenario 3 we address the transport and fate associated with the reverse estuarine circulations (Fig. 4b). Reverse estuarine circulations exist in Kuwait Bay in the NW Gulf. Near the surface, relatively low-density waters enter the Bay and eventually sink due to an increase in the salinity and therefore density as a result of evaporation during summer and desalination plants discharges (Alosairi et al., 2018b). Although the vertical and horizontal density gradients are not excessive, there is seaward residual near the bed of the order of 20 cm s^{-1} during neap tide conditions in summer (Fig. 4b) (Alosairi et al., 2018b). The residual currents seem to play a key role in the distributions of various substances in the area, via the deeper channels, to the Gulf. As for the particulate matter, it acts as an exporter from the Bay to the Gulf, and is assessed for MPs in this Scenario.

To elaborate on Scenario 3, for many years littering in Kuwait Bay has been one of the highest in the region due to the dense population that surrounds it and the urbanisation on and near the coastline. This is believed to go hand in hand with the increase in MPs transport to the marine environment (Naji et al., 2017b). Furthermore, future construction and extension of urbanisation in the northern part of the Bay are expected to produce more plastic solid waste and increase primary MPs sources (Westall and Hagagy, 2019). Throughout the southern coast of the Bay, both JH and SL release sites are considered to be key

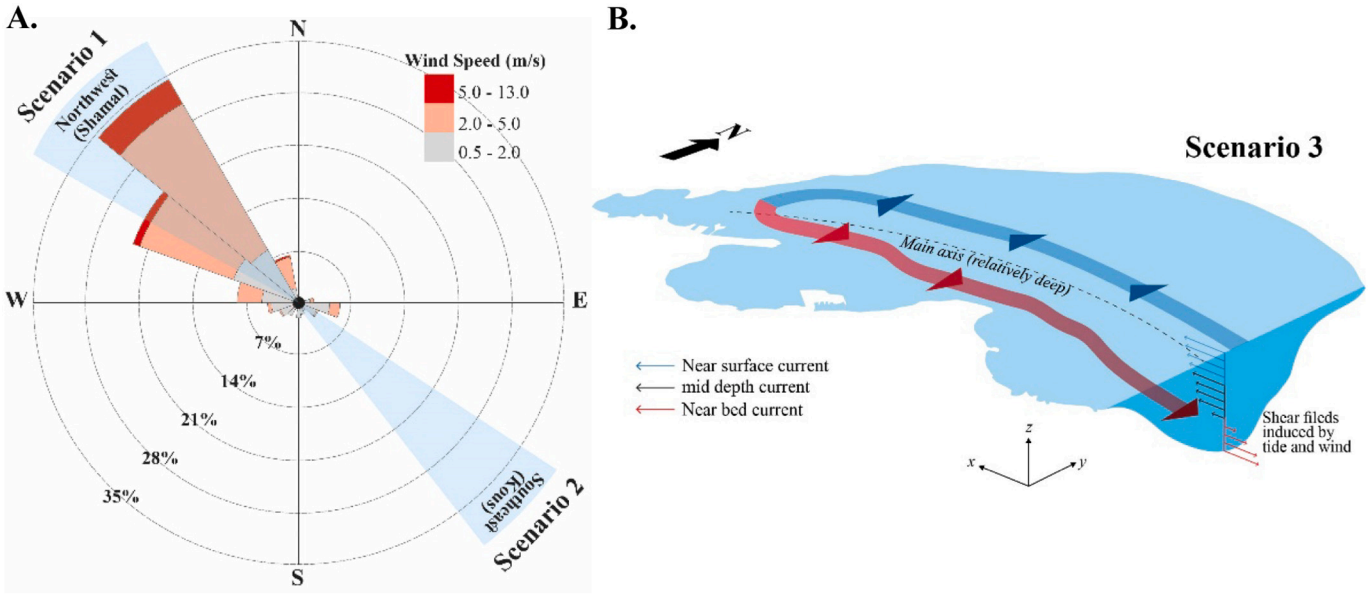

Fig. 4. Demonstration of the physical forcing associated with the numerical scenarios (a) wind conditions, obtained from Alosairi and Alsulaiman (2020) (b) reverse estuarine conditions in Kuwait Bay.

Table 3
The baseline numerical settings including parameter sensitivity assessment of Delft3D-PART.

Parameter	Values	Comments and justification
Diffusivity	5, 10, and 20 $m^2 s^{-1}$	Mixing at the horizontal scales less than the computational grid was parametrized by a turbulent diffusion coefficient as explained by Okubo (1971). For shallow areas like the NW of the Gulf, its believe to range 5–20 $m^2 s^{-1}$. A value of 10 $m^2 s^{-1}$ was adopted as a standard value (Alosairi et al., 2011)
Number of particles per release	1000, 3000, and 5000	To ensure the divergence of the solutions several particle counts were used which are in-line with past research (Núñez et al., 2019). The best fit computationally and physically is 1000 per release point (for baseline, scenario 1 and 2) and 2000 for scenario 3 (divided equally between surface and bed releases).
Mass per release	1000, 3000, 5000 kg	For simplicity and readability of the concentration of the particles the mass selected in the study 1000 per release which correspond with the number of particles being selected.
Wind drag	1%, 3%, 5% and 6%	In studies that include wind drift, the value of the wind drift coefficient varies from 1% (Ebbesmeyer et al., 2012) to 6% (Maximenko et al., 2015), and in some studies a range of values are used or the value used is not given but instead the empirical formula for calculating the wind drift is given (Kako et al., 2010). In the case of submerged plastic debris, it is spread through the water column, with no exposure to the wind and hence no wind drift is assumed (Reisser et al., 2013).
Beaching probability	0.1, 0.5, and 0.7	Beaching of MP are considered to be smaller for micro scale compared to the macro scale on the basis given in (Hinata et al., 2020). It was found that 0.1 is most representative value for the MP.
Density of particle	918, 920, 952, 950 kg m^{-3}	Based on average PSW densities determined experimentally in Al-Salem et al. (2015) for plastic film waste that could fragment and be rendered as MP in Kuwait. The chosen density is the average polyolefin (polymer) that prevails in conversion processes which is as per the distribution of PSW determined thus (wt%): linear low density polyethylene (LLDPE, 46%), low density polyethylene (LDPE, 51%), high density polyethylene (HDPE, 1%) and polypropylene (PP, 2%) (Al-Salem, 2019b). For the current study the 920 kg m^{-3} was used since it represents the highest percentage of the polymer.
Release tidal phase	High and low tides (neap spring)	The release was made during the high slack tide.
Model (run) time step	1,5 and 10 min	This is to ensure the divergence of the solutions and suitable computational time, the time step of 5 min was found to be best fit.

source release points for marine litter that eventually finds its way to the vicinity of the reverse estuarine fields (Fig. 4b). In the event that litter gets trapped in the seabed, particularly in the deep portions of the Bay, it acts as a source of micro- and macro-plastics after abrasion and physical fragmentation (Al-Salem, 2019a). Hypothetically, over years this should represent a persistent source in the NW Gulf. Therefore, in Scenario 3 MPs should be released at the surface and near the bed, with these particles acting as tracers, and windage effects negligible near the bed.

2.7. Particle tracking model configuration, sensitivity and limitations

The behaviour and mobility of MPs depend significantly on particle size, and to a smaller extent on the density of the receiving waters. As a plastic particle decreases in size its buoyancy is reduced, and so its position within the water column is controlled more by the local dynamics. Plastics at and below micro scale exhibit colloidal particle behaviour and exist mainly as suspended particles in the turbulent water column, where their densities become irrelevant (Filella, 2015), but during relatively calm conditions or in along-shore flow, MPs float on the surface. In the current study we consider the particles to be on surface for Scenarios 1 and 2, while for Scenario 3 additional releases were made near the bed to cover many case studies. As we have seen, the full 3D behaviour of MPs is complex and beyond the scope of the current study.

Other factors that control the behaviour of MPs during the initial stages after release are the number of particles, release time, diffusivity, and windage. Since there is limited published literature reporting the values of the numerical parameters (which are included in Table 3 along with the input data) sensitivity assessments were the best approach to set the input parameters. As the factors and the unknowns are highly variable and there are endless combinations of conditions assessing these, it is important to limit the varying parameters carefully so they remain representative of the real environment. The aim of sensitivity assessment is to identify the most important parameter controlling the transport and distributions of MPs. Initially, the variations of the parameters were selected from the literature or by doubling the standard values and monitoring the effects on the particles (Stuparu et al., 2015; Martin et al., 2019; Politikos et al., 2020).

The sensitivity assessment revealed that the different combinations of the parameters in Table 3 lead to different transport conditions in the initial stages, while the windage parameter had the most effect on the transport particularly in the offshore region. The diffusivity parameter did not show significant difference in the scale of the particle patch once released, remaining almost the same for 5, 10, and 20 $m^2 s^{-1}$. Since this parameter accounts for the turbulent diffusion at the sub-grid scale, and given the shallowness of the area, the value of 10 $m^2 s^{-1}$ was found reasonable for the NW Gulf and agrees well with the findings of Alosairi et al. (2011). As for the number of particles, high number favour greater statistical certainty in the random-walk method. However, large number of particles would require large computational times. A test was conducted with 1000, 3000 and 5000 particles per site, showing that 1000 is reasonable for the purpose of the study to represent the transport regime of the MPs while maintaining reasonable computational time. Assessments of 1000 and 3000 particles per site revealed an almost identical distribution but there were higher concentrations of particles for the 3000 particles case. For simplicity and readability of the results the mass per release was set to 1000 kg, matching the number of particles being released from each location. It is worth noting that the mass would have negligible effect on the behaviour of the MPs if it is assumed no decay or settling occurs. The windage parameter has been assessed for sensitivity by setting four conditions, of 1, 3, 5, or 6%. The higher the value the greater drag occurring, and therefore the greater transport of particles. Reisser et al., (2013) assessed the submerged plastic transport by neglecting the wind effects, while other studies suggested using an empirical formula (Kako et al., 2010). As MPs are normally found at the surface and mostly submerged, in the current study the windage parameter were set to the lowest value, 1%, to represent a low drag force. In practice marine plastics, including MPs, experience three processes close to the shoreline: beaching, stranding, and backwashing (Hinata et al., 2020). From size-dependent behaviours of plastics in coastal regions it can be assumed that the larger the size and specific density the more trapping and longer residence times are expected (Hinata et al., 2020; Isobe et al., 2014). As far as the MPs are concerned, in the current study the beaching probability is set to the minimum 0.1 indicated in Table 3, as they have less tendency to beach than larger plastic sizes. Although some regions could experience long residence times along the beach at

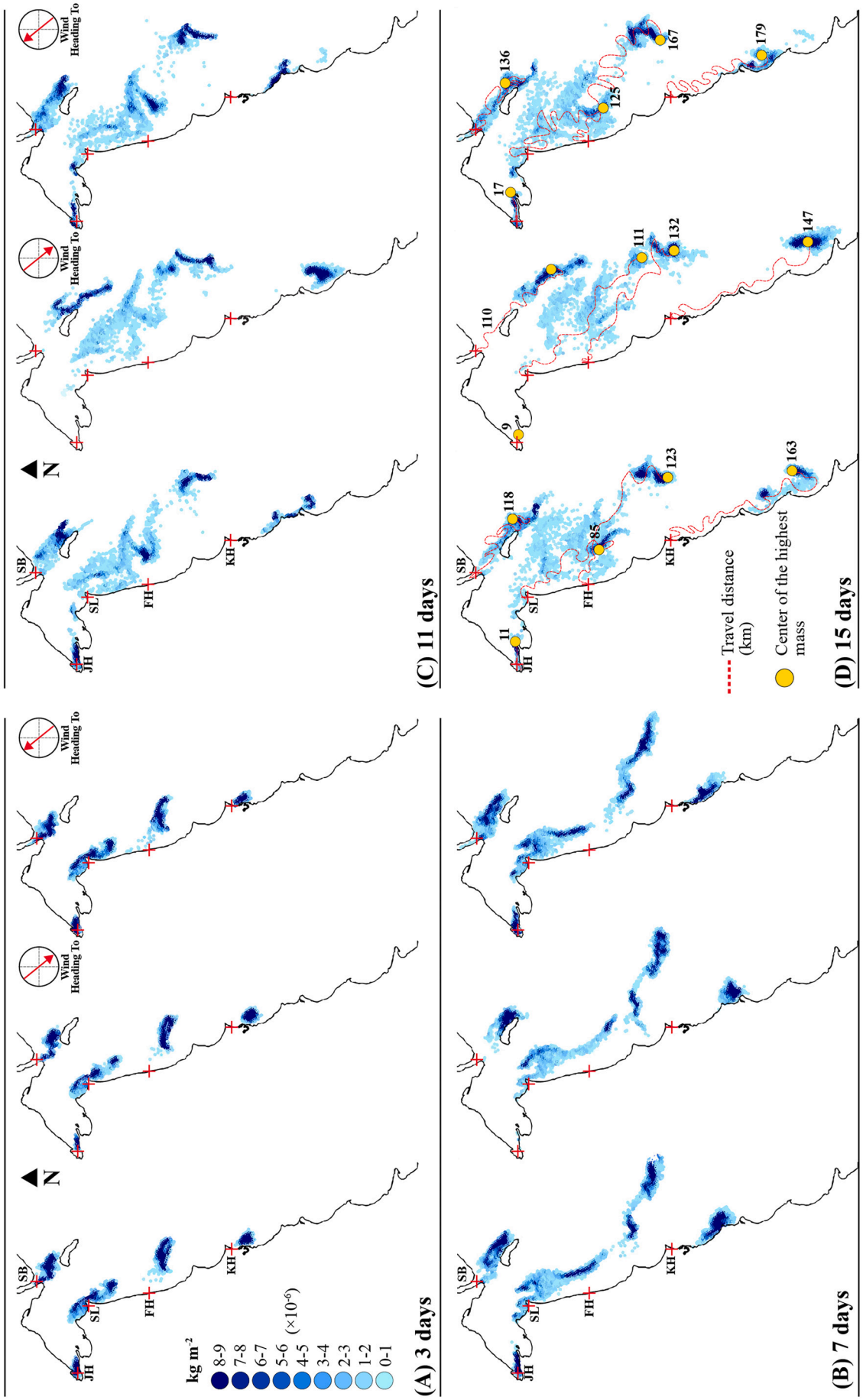

Fig. 5. The distributions and trajectory of MP (represented as a mass) release from the key locations after (a) 3 days, (b) 7 days, (c) 11 days; and (d): 15 days.

MP scale, this is still an area requiring research in the Gulf. It is noteworthy that the sensitivity assessment revealed that beaching probability has a large effect on the concentration and the quantities of particles being transported, particularly when set to 0.7.

The momentum associated with the ambient flow, particularly nearshore, plays a significant role in the transport due to the large differences in density that cannot be resisted at a micro scale. Perhaps in regions closer to Shatt Al Arab where the ambient density is comparable to the MPs density this parameter becomes more relevant. The sensitivity assessment revealed that the transport behaviours of MPs varying in density from 918 to 950 kg m^{-3} were similar. As to timing of release with respect to tidal phase, the particles were released during the slack conditions at high tide to avoid the instant beaching which occurs when the particle is released during the slack of low tide. Lastly on the sensitivity of the model, test computations were conducted to ensure a suitable time step for the particle tracking model and convergence behaviour of particles. We found that a timestep of 5 min resulted in reasonable computational times. This exercise was carried out to ensure the best representative conditions of the studied environment on the one hand, and to avoid high computational cost and numerical instabilities on the other. The values selected in Table 3 represent the Baseline conditions.

It is important to address the limitations of the numerical techniques and assumptions made in studying the transport and fate of the MPs. In the current study our focus has been the intermediate-term transport, of the order of 15 days, estimating transport timescales and distributions at intermediate fields. At near fields the effects of wave and coastal interactions are more complex and require further research. These processes may affect the concentrations of the MPs in many ways, including the beaching which has been simplified in the current study. At far fields, particle tracking methods may not serve a useful purpose as enormous numbers of released particles would be required to provide a representative model, and so extensive computational capacity would be required. It should also be noted that physical processes involved in breaking down and degrading MPs have not been considered in the current work. At large temporal scales MPs undergo complex combinations of several processes including mechanical breakdown, degradation and biofouling. This should lead to shifts in their physical properties that gradually modifies their density and affects their behaviour within the water column, as previously explained by Morét-Ferguson et al. (2010). In this context biofouling leads to an increase to the density of the plastics while the reduction in buoyancy leads to sinking in a combined effect with a clear impact on transport modelling results. Floating MP particles along with other plastic marine litter are susceptible to extensive fouling which is defined as covering the surface of the plastic resin with a biofilm followed by an algal mat and then a colony of invertebrates (Muthukumar et al., 2011). The rate of biofouling depends on the surface energy of the plastic resin which is between 5 and 25 mN m^{-1} as previously described by Andrady (2011). Such a behaviour will lead to MP particles to sink in getting encrusted with foulants which increases its density (Andrady, 2011; Kaiser et al., 2017; Zhang, 2017). Such a phenomena is likely to prevail in bioactive regions such as Sulaibikhat and Jahra Bays. This is a complex process that requires further research and extensive efforts to obtain suitable empirical representation for modelling purposes.

3. Results and discussion

In coastal regions where MPs are released, the combination of high tidal range and shallow waters results in strong nearshore currents that supports their dispersion. Other key drivers for MPs distribution are the hydrodynamics comprising several physical forcing factors including winds, tides and (at longer time frames) density gradients, with the interchanging combination of forces governing the distribution, concentration, and the transport of microplastic particles. With this basis, the results of the Baseline conditions and the numerical Scenarios considered in the study are indicated in Fig. 5. The elapsed time from the release up to the end of the simulation has been tracked for all cases and release locations, while a snapshot has been taken after 3, 7, 11 and 15 days (Fig. 5). This demonstrates the near-coast progress of the particle patches as well as the intermediate transport fields.

In general, the results of the simulations other than from the JH release point demonstrated a progressive transport towards the southern area of the Gulf (Fig. 5d). This is generally assisted by the transport regime of the region shown in Figs. 2 and 3. During the first three days in SL, FH, KH, and SB, the cloud of the particles grows dependent on the nearshore dynamics which is mainly governed by the tides, while winds have a lesser role in stretching the patch of particles. This is evident from the results of the Baseline conditions, Scenarios 1 and 2, which were comparable in terms of patch size and concentrations during the first 3 days (Fig. 5a). The tidal forces result in a large shear deformation of the patch which aids transverse dispersion, and most likely, it would increase the fragmentation in the long run. During the initial days of the baseline conditions, the patch of the particles further stretches along the shoreline which demonstrate the tidal effects (Fig. 5a). Wind effects are mostly evident in the JH release, which is restricted in nature, compared to the other release locations. In Scenario 1 at JH, the Shamal wind acts to impose additional shear stresses at the surface that result in narrow and concentrated offshore particle patches highly interactive with the coastline. As a result, the MPs are spread extensively along the southern shore of Jahra Bay and Doha. In contrast the Scenario 2 Kous winds resulted in opposite effects, wide spreading towards the offshore which covered most of Jahra Bay (Fig. 5a). In SL, the Shamal winds largely control the distributions of the MPs. The combined effects of the turbulence at the headland and the Shamal wind shear allow for immense dispersion and southeast transport during the first 3 days (Fig. 5a). As a result, lower concentrations are associated with the SL release than with the other releases. Although similar dynamic features prevail during the Baseline and Scenario 2, neither results in shear fields as large as those in Scenario 1. At SB and KH the winds of Scenario 1 and 2 act only to advect the MPs cloud southward and northward, respectively. This is evident from the concentration of the patches from these release locations. At SB, the northward transport allows MPs to enter the Subiya channel, while the southward transport heads towards Failaka Island where further interactions with the coastline are achieved. At KH the Shamal wind allowed for along-shore transport and the Kous wind delayed the later effects.

Seven days after the release the effect of the winds is more apparent than the tides in transporting MPs (Fig. 5b). At the SB release point the particles are further advected due to Shamal winds of Scenario 1 and are more in Scenario 2. It is worth noting that although the Shamal wind evidently assists the transport, the Kous (southern) winds contribute greatly to the lateral dispersion of MPs. The MP cloud is widely distributed during Kous winds compared to Shamal in SB (Fig. 5b). In the same context, the concentration of MPs in Scenario 2 is slightly less in SB compared to Scenario 1. This can be attributed to the initial trapping of the particles in Khor Al-Subiya and the dominant flow divergence associated with the Kous wind in Scenario 2. The wind role in the vicinity of SB is more pronounced due to the shallow nature of the area. Another key observation at this stage is the disappearance of the particles from the JH release in Scenario 1 (Fig. 5b). The Shamal winds resulted in trapping and beaching most of the microplastic particles in Jahra Bay and along the southern coastline near Doha. Due to the hydrographical nature of Jahra Bay, particularly shallow and semi-enclosed, the particles did not progress towards the main channel of the Bay.

Amongst all the release points, the roles of eddies and horizontal dispersion are found to be prominent at SL after 7 days (Fig. 5c). As soon as the MP patch reaches the headland of Salmiya, the eddies depicted in Fig. 2 played a significant role in large scale dispersion, enhanced by shear forces. The horizontal distribution of MPs seems to be

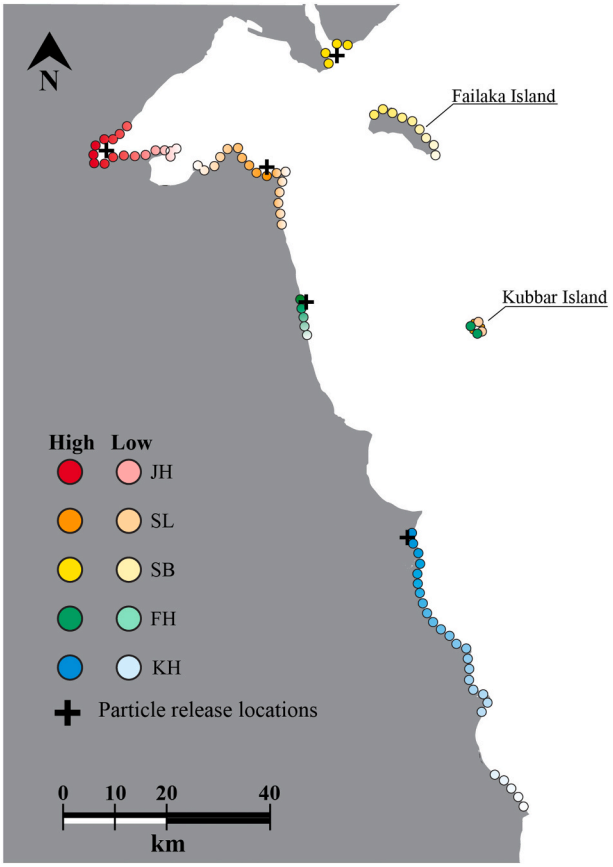

Fig. 6. Beached particles after 15 days from the five release locations during the baseline conditions.

independent of the wind conditions for all the Scenarios in SL due to the wide turbulent fields created by Salmiya headland. As a result, the concentration of the MPs was significantly reduced after 7 days, particularly for the Shamal wind case which transported the particles further southward by about 10 km compared to the other cases.

Although the coastline alignment and hydrographical nature are similar at the southern coast releases of FH and KH, two different transport behaviours were noted in this work. In FH, the dispatch of the MPs away from the coastline by 5 km is achieved after 7 days (Fig. 5b). However, in KH the transport continues along and attached to the coastline (Fig. 5b and c). It could be said that the main reason for such behaviour are the coastline hydrographical characteristics. At the FH release point a steep bathymetric profile characterizes the coast, where the depth reaches more than 15 m within 1.5 km from the coastline (Fig. 3e). This allows for flow streamline divergence associated with larger water volumes that drift away from the coastline. In contrast the release of MPs in KH is within wider shallow regions (Fig. 3f), and therefore the along-shore currents act on wider fields. From a wind regime perspective, the Shamal wind enables further advancement of the MPs at KH until it reaches a relatively deeper region where it has been dispatched off the coastline near Saudi Arabia after 15 days (Fig. 5d). However, for the FH release site, Shamal winds do not have significant effects on the southward transport but rather on the horizontal distribution of the MPs where the concentrations are reduced (compare Fig. 5c and d). This is attributed to the direction of the Shamal wind which act across the strong seaward flow fields, and therefore, enables the spreading of the particles. As for the Kous winds at KH, progress of the particles is slowed after 11 days of the release, due to the opposing effects between the wind and the ebb-dominant current (Fig. 5c). In the same Scenario after 15 days of the FH release, the particles were concentrated, indicating less horizontal distribution occurred due to the Kous winds compared to Shamal (Fig. 5d). Amongst all conditions and release locations, the transport process in FH was most significant and dispersion the least during Scenario 2 (see Fig. 5d).

Between 11 and 15 days after release, the transport regime does not shift dramatically. However, it is worth considering the particles of JH in the semi-enclosed region. The Kous winds in particular enable the patch to be transported slightly further seawards than the Baseline conditions (Fig. 5d). Although the transport in these circumstances is least in terms of distance compared to other releases, further transport can be achieved when MP patches reach the reverse estuarine fields of the Bay (shown in Fig. 4b). The reverse estuarine circulations at the main channel of the Bay are known to export material via the lower layer to the offshore.

To further investigate the transport of MPs, the travel distance of the masses has been computed at the end of the simulation for all the given Scenarios and release locations (Fig. 5d). The computation of the travel distance was obtained by tracking of the highest concentrations within an area of 25 km^2 throughout the simulation period. In general, the results indicated that the longer travel distances are not necessarily associated with the Shamal, although these patches are found at farther distances than in other conditions. The Kous winds enable the concentrated patches to fluctuate more than the Shamal winds, that resulted in longer travel distances (Fig. 5d). The trajectories are comparable for the Baseline conditions and the Kous, but in the latter longer distances are travelled. The results here also indicated that the Shamal winds are relatively effective in delaying the advancement of the particles towards the north. The results revealed that the highest travel distance was achieved in the KH release of Scenario 2. This is when the along-shore transport is well defined with dominating movements of particles back and forth resulting in high travel distance. The travel distance of the JH release is comparable for all of the study cases. This emphasises the effects of the enclosed regions in trapping the MPs, and inhibiting advance to greater distances, so long MP retention times can be found in those regions. As seen in Fig. 5, the transport particularly varies during large temporal scales based on the forcing conditions; nearshore the beaching of particles is less affected by these forces. Therefore, we include the beached MPs results during the Baseline conditions in Fig. 6 and compute the percentages of beached and floating particles in Table 4.

The distribution of the beached MPs at each release site provides further insight into the nearshore dispersion and fate of the MPs (Fig. 6). In the enclosed area of Jahra Bay, the MPs covered most of the shoreline including the Doha area as depicted in Fig. 6. It was estimated that more than half of the particles were beached during the Baseline

Table 4
The percentage of the masses being beached and transport for the Baseline conditions (BL), Scenario 1 (S1), and Scenario 2 (S2).

Release location		**JH**			**SL**			**SB**			**FH**			**KH**	
Scenario	BL	S1	S2	BL	S1	S2	BL	S1	S2	BL	S1	S2	BL	S1	S2
Floating mass	42%	5%	39%	73%	76%	69%	85%	78%	80%	98%	93%	90%	67%	73%	54%
Beached mass	58%	95%	61%	27%	24%	31%	15%	22%	20%	2%	7%	10%	33%	27%	46%

conditions and almost all of the particles were beached during the Shamal winds Scenario (Table 4). It is thought that Sulaibikhat Bay would share similar distribution behaviour under similar circumstances: these areas are favourable for trapping due to their semi-enclosed nature. In contrast, much wider spreading of beached particles is achieved at SL stations (Fig. 6). The eddy associated with the Salmiya headland results in wide spreading in which particles were found to remain along most of Kuwait City coast and reach up to Kubar Island, but in low concentration. Although wider spread of beached particles are achieved, they are in low mass concentration since most of the particles are in a floating state in SL under all conditions (Table 4). The widely-spread beached MP particles are estimated to cover a length of 66 km, which is the highest amongst the northern releases (Fig. 6). The beaching of MPs was confirmed by the research team of this work using the KISR-research drone to visually verify the beaching and MPs accumulation from JH site shown in Fig. 6. We report in Figs. S2 images captured from various heights alongside coastal images of MPs and marine litter that is beached along the coastline, believed to be from both JH and SL sites as well as Kuwait City area, which has circulated along the Bay area, namely the Shuwaikh. At the southern coast, FH is found to have the highest percentage of floating particles (Table 4), again confirming the earlier findings where the particles are swiftly transported offshore, so beached particles are lowest in FH. The KH release adopted similar beaching-to-floating ratios to FH, but the key difference is found in the Kous wind conditions. Almost half of the mass was found to be beached along the coast in KH (Table 4). This is mainly associated with the along-shore currents that maintained the coastal interactions throughout the studied period. It is worth noting that high concentrations of MPs were found beached in Kubar Island associated with FH release, endorsing the strong seaward transport. The highest distribution of MPs was found in the KH release which demonstrated a classical along-shore transport (Fig. 6). The beached particles stretched along 70 km of the coastline, which may extend beyond the simulation area. However, the concentration of the beached particles reduces as one moves southwards away from the release location (Table 4).

MPs released from SB site were found to be beached at the headland of Subiya and Boubyan Island (Fig. 6). The initial particle distribution, assisted by the tidal pumping of Khor Al-Subiya, resulted in jet-like spreading that eventually hugged the northern shoreline of Failaka Island where high concentrations were found (Fig. 6). Also, it must be noted that some particles were trapped within Khor Al-Subiya but at low concentrations that could not be detected well with the current resolution of the numerical grid (Table 4). In addition, the masses of beached particles in all Scenarios vary minimally in SB. That being said, the locations of the release could strongly govern the distributions of the particles in Khor Al-Subiya. It is known that the circulations are remarkably high (with tidal currents exceeding 0.9 m s^{-1} during spring tides), but due to the nature of the area which includes a tidal divide near the middle of Khor Al-Subiya channel, more beached particles could be expected due to trapping (Alosairi et al., 2018a).

Holistically, the total floating and beached masses has been computed for all of the sites and conditions throughout the simulation period (Fig. 7). In general, the results of this study revealed that the transport of MPs in the NW Gulf reach a steady state in roughly 15 days. This is evident from the floating masses during all of the conditions

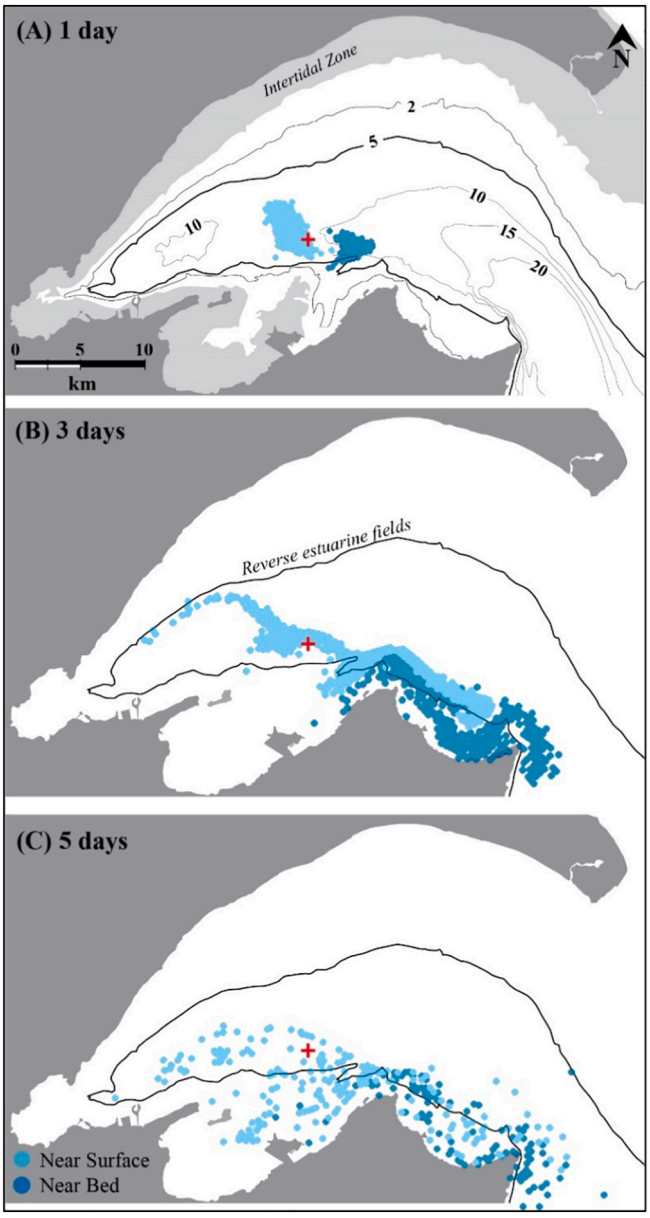

Fig. 8. Particle distributions due to reverse estuarine circulations in Kuwait Bay.

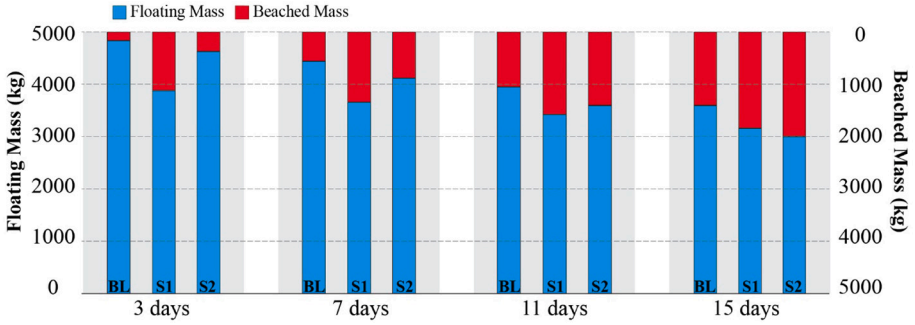

Fig. 7. Total beached and floating masses for all the release locations for the baseline, Scenario 1 (S1), and Scenario 2 (S2).

after the 11 and 15 days which are comparable. Thereafter, the results suggest that the floating particles would reach farther distances and beaching would cease. It is also notable that the Shamal winds, indicated as S1 in Fig. 7, result in high beaching during the early days of the release compared to the other conditions, this is perhaps more pronounced in Kuwait Bay. The overview indicated that the releases are predominantly in transport and dispersive mode rather than beaching which only accounted for about quarter of the total masses in all Scenarios collectively.

The results of Scenario 3 associated with the reverse estuarine circulations are shown in Fig. 8. The particle transport and dispersion for the elapsed times of 1, 3 and 5 days are also shown in the same Figure. The results include the simultaneous particle release at the surface and near-bed within the reverse estuarine fields. During the first day of the release, the effect of the reverse estuarine circulations was noticed immediately. The particle patch grows in size due to the tidal shear stresses, until it reaches a diameter of about 2 km (Fig. 8a). Thereafter, the reverse estuarine fields are large enough to capture the plume of MP particles and take over the role of transport and well as the longitudinal dispersion (Fig. 8b). The near-bed particles progressively move seawards while the near-surface particles head landwards (Fig. 8b). The longitudinal dispersion assisted by the vertical density gradients as well as the tidal shear results in further stretching of the MP particles cloud until it extends to essentially the full length of the Bay (Fig. 8b). However, the distributions of the particles are based on the vertical orientations of the release. The MP particles occupy the western coast of the Bay while the eastern side is dominated by the near-bed particle release. Progressively, the MP particles are transported southward, due to the dominant northern Shamal winds, and embrace the shoreline of Kuwait City (Fig. 8c).

At the headland of Kuwait City, mixed particles of surface and bed releases were found. This demonstrates the effects of the eddies in the region which are mainly generated by tides. As a result, the patch of MPs is swiftly distributed and dispersed along the coastline. By then, the along-shore current takes over the role of the transport towards the sea in a trickling mode to the NW of Gulf (Fig. 8c). In contrast for the surface release, the particles are within the main channel but do move landwards with far fewer interactions with the coastline (Fig. 8b). The enclosed regions of Jahra and Sulaibikhat Bays with their narrow and relatively deep entrance (~7 m on average) allow tidal pumping, as explained previously by Fischer et al., 2013. This has allowed for transverse dispersion that eventually leads MP particles to be trapped as detailed by Alosairi et al. (2011) and Pokavanich and Alosairi, 2014 (Fig. 7c). At this stage, particles within the shallow coastal regions, where depth becomes irrelevant and vertical density induced circulations are negligible, the along-shore current provides the transport. Evidently, associated with the particle release locations, the particles are beached at the southern coast of the Bay.

It is noteworthy that the reverse estuarine circulation within the Bay is mainly associated with the neap conditions during summer (Alosairi and Pokavanich, 2017). Other circulation pattern may differ seasonally for the same water body. This is due to the baroclinic settings of the shallow waterbodies which are responsive to the climatic conditions. In the case of the Bay, the Shamal winds advect pollutants southwards. In slower transport modes it is important to mention that the reverse estuarine circulations vary in extent. In seasons of high freshwater discharges from Shatt Al-Arab (Fig. 1) higher reverse estuarine circulations are expected in the Bay (Alosairi et al., 2019). This should enhance the exchange rate between the Bay and the NW Gulf via higher inflows from the surface to the Bay and outflows from the Bay into the NW. Therefore, an interannual transport regime of MPs is anticipated. In the same context, but not studied here, the discharges from Shatt Al Arab are more likely associated with varying size of plastics due to the upstream dense human activities. In a scenario of Mesopotamian Marshes recovering from desiccation and of regulating dam construction, high flows are expected from Shatt Al-Arab (Alosairi et al., 2018a, 2018b). In addition, sudden and intense rainfall should also recharge the catchments and increase the flow through Shatt Al-Arab (Alosairi et al., 2019). Correspondingly, the reverse estuarine circulations should import MPs into the Bay from the surface as they are likely be found within Shatt Al Arab discharge. Studying this aspect is complex and requires further understanding of the estuarine fields near the discharge as MPs could be trapped at saline fronts similar to the ones found in Rio de la Plata estuary in Brazil (Acha et al., 2003). The numerical assessments of MPs behaviour, including the land-based releases and the wind force controls of this study, reveal the dominant patterns, trappings, and trajectories of the MPs. The assessment has enabled the construction of the MPs transport regime of the NW Gulf illustrated in Fig. 9. In general, within the Bay borderlines, the trapping zones of Sulaibikhat and Jahra Bays maintain higher residence times for the particles. This also supports the fact that the majority of fish species having MP particles in their gut contents are typically caught within the Bay (Al-Salem et al., 2020b). The ebb-dominant tidal conditions along the shore of Kuwait aided by the Shamal winds result in high shear fields compared to the Kous winds, and therefore greater distribution are achieved.

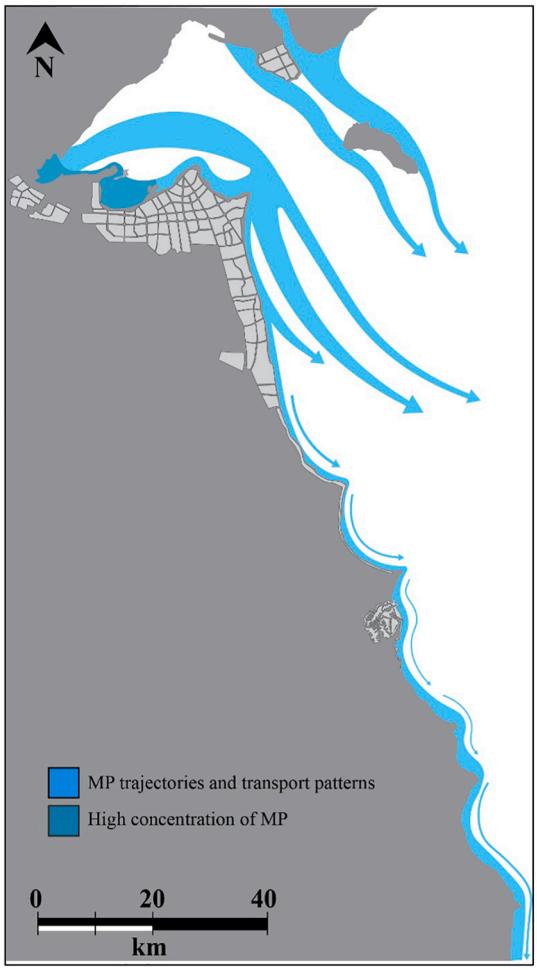

Fig. 9. Microplastic trajectories and transport patterns at the NW of the Arabian Gulf.

4. Conclusion

Enclosed seas are typically associated with high densities of marine litter on the seafloor. The Gulf is not very different from other enclosed sea bodies such as the Mediterranean and the Black Seas due to its semi-enclosed nature, high residence times, and the relative human activities

along the coast. To reach a firm conclusion an extensive collaborative effort particularly in the monitoring and detailed measurements campaign is required. In the current study numerical model simulations have been utilized to understand and evaluate the transport regimes and distributions of MPs at the NW Gulf. The numerical assessments of the MP behaviour, including the land-based releases and the wind force studies, reveal the dominant patterns, trappings, and trajectories of the MPs. This assessment has enabled construction of the MP transport regime of the NW Gulf. In general, the trapping zones of Sulaibikhat and Jahra Bays maintain higher residence time for the particles compared to open areas. This is also supported by the fact that typically fish species with MP particles in their gut content are caught within the Bay. The ebb-dominant tidal conditions along the shore of Kuwait aided by the Shamal winds result in high shear fields compared to the Kous winds, that showed wider distribution for plastic particles. In general, the NW Gulf acts as supplier to the remaining Gulf southern regions of the open areas. The dispersion of the MP plume after 15 days as discussed in the numerical Scenarios complement information based on the type of marine fish that were characterized and found to possess MP particles within their gut contents. Based on previous experimental work conducted in Kuwait, fish near and inside the Bay area are susceptible to uptake of MPs. The findings of this study can be used as an opportunity to integrate the different types of indicators to take into account the socio-economic and environmental impacts that result from MP littering. The realization of the magnitude of the mismanagement of PSW will lead to the re-evaluation of the current management policies. This also prompts authorities to take these findings into account when framing laws in Kuwait to control waste and marine litter sources around the Bay area.

CRediT authorship contribution statement

Y. Alosairi: Data curation, Formal analysis, Writing - original draft, Writing - review & editing. **S.M. Al-Salem:** Conceptualization, Writing - original draft, Writing - review & editing. **A. Alragum:** Writing - review & editing.

Declaration of competing interest

The authors of this communication declare that they have no known competing interests or personal relationships that could influence the work in any shape or form.

Acknowledgment

The authors would like to thank the Kuwait Institute for Scientific Research (KISR) for their support towards this work.

Appendix A. Supplementary data

The article contains a Supplementary material file that can be found on the journal's website. Supplementary data to this article can be found online at https://doi.org/10.1016/j.marpolbul.2020.111723.

References

Abayomi, O.A., Range, P., Al-Ghouti, M.A., Obbard, J.P., Almeer, S.H., Ben-Hamadou, R., 2017. Microplastics in coastal environments of the Arabian Gulf. Mar. Pollut. Bull. 124, 181–188.

Abbasi, S., Soltani, N., Keshavarzi, B., Moore, F., Turner, A., Hassanaghaei, M., 2018. Microplastics in different tissues of fish and prawn from the Musa Estuary, Persian Gulf. Chemosphere 205, 80–87.

Acha, E.M., Mianzan, H.W., Iribarne, O., Gagliardini, D.A., Lasta, C., Daleo, P., 2003. The role of the Rio de la Plata salinity front in accumulating debris. Mar. Pollut. Bull. 46, 197–202.

Akhbarizadeh, R., Moore, F., Keshavarzi, B., Moeinpour, A., 2017. Microplastics and potentially toxic elements in coastal sediments of Iran's main oil terminal (Khark Island). Environ. Pollut. 220, 720–731.

Al-Husaini, M., Bishop, J.M., Al-Foudari, H.M., Al-Baz, A.F., 2015. A review of the status and development of Kuwait's fisheries. Mar. Pollut. Bull. 100, 597–606.

Aliabad, M.K., Nassiri, M., Ko, K., 2019. Microplastics in the surface seawaters of chabahar bay, Gulf of Oman (Makran coasts). Mar. Pollut. Bull. 143, 125–133.

Alosairi, Y., Alsulaiman, N., 2020. Hydro-environmental processes governing the formation of hypoxic parcels in an inverse estuarine water body: assessment of physical controls. Mar. Pollut. Bull. 157, 111311.

Alosairi, Y., Pokavanich, T., 2017. Seasonal circulation assessments of the northern Arabian/Persian Gulf. Mar. Pollut. Bull. 116, 270–290.

Alosairi, Y., Imberger, J., Falconer, R.A., 2011. Mixing and flushing in the Persian Gulf (Arabian Gulf). Journal of Geophysical Research: Oceans 116 (C3).

Alosairi, Y., Pokavanich, T., Al-Salem, K., Taqi, A., Al-Said, T., Al-Hashem, A., Al-Rubaiaan, E., Karam, Q., Al-Yaegoub, A., Al-Dousari, N., Al-Awadhi, S., Al-Houti, D., Shuhaibar, B., 2015. The Optimal and Sustainable Extension of the Emergency Outfalls Along Kuwait Coastline. Kuwait Institute for Scientific Research, Report No. KISR 12782.

Alosairi, Y., Alsulaiman, N., Neelamani, S., Polikarpov, I., Kwarteng, A., Small, C., 2018a. Effects of developments in Mesopotamian Marshland on Boubyan and Warba Island. In: Kuwait Institute for Scientific Research, KISR Report No. 14765.

Alosairi, Y., Pokavanich, T., Alsulaiman, N., 2018b. Three-dimensional hydrodynamic modelling study of reverse estuarine circulation: Kuwait Bay. Mar. Pollut. Bull. 127, 82–96.

Alosairi, Y., Alsulaiman, N., Petrov, P., Karam, Q., 2019. Responses of salinity and chlorophyll-a to extreme rainfall events in the northwest Arabian Gulf: emphasis on Shatt Al-Arab. Mar. Pollut. Bull. 149, 110564.

Al-Qassimi, M., Al-Salem, S.M., 2020. Ambient levels as a secondary airborne precursor in Fahaheel urban area, the State of Kuwait. Atmospheric Science Letters 1–14.

Al-Salem, S.M., 2019a. Introduction. Chapter 1. In: Plastics to Energy: Fuel, Chemicals, and Sustainability Implications, 1st edition. Elsevier, pp. 3–20. https://doi.org/10.1016/B978-0-12-813140-4.00001-7. ISBN: 978-012813140-4;978-012813141-1.

Al-Salem, S.M., 2019b. Influential parameters on natural weathering under harsh climatic conditions of mechanically recycled plastic film specimens. J. Environ. Manag. 230, 355–365.

Al-Salem, S.M., Abraham, G., Al-Qabandi, O.A., Dashti, A.M., 2015. Investigating the effect of accelerated weathering on the mechanical and physical properties of high content plastic solid waste (PSW) blends with virgin linear low density polyethylene (LLDPE). Polym. Test. 46, 116–121.

Al-Salem, S.M., Uddin, S., Lyons, B., 2020a. Evidence of microplastics (MP) in gut content of major consumed marine fish species in the State of Kuwait (of the Arabian/Persian Gulf). Mar. Pollut. Bull. 154, 111052.

Al-Salem, S.M., Al-Nasser, A., Al-Dhafeeri, A.T., 2018a. Multi-variable regression analysis for the solid waste generation in the State of Kuwait. Process Safety & Environmental Protection 119, 172–180.

Al-Salem, S.M., Bumajdad, A., Khan, A.R., Sharma, B.K., Chandrasekaran, S.R., Al-Turki, F.A., Jassem, F.H., Al-Dhafeeri, A.T., 2018b. Nonisothermal degradation kinetics of virgin linear low densitypolyethylene (LLDPE) and biodegradable polymer blends. J. Polym. Res. 25, 111.

Al-Salem, S.M., Uddin, S., Al-Yamani, F., 2020b. An assessment of microplastics threat to the marine environment: a short review in context of the Arabian/Persian Gulf. Mar. Environ. Res. 159, 104961.

Al-Sarawi, H.A., Jha, A.N., Baker-Austin, C., Al-Sarawi, M.A., Lyons, B.P., 2018. Baseline screening for the presence of antimicrobial resistance in E. coli isolated from Kuwait's marine environment. Mar. Pollut. Bull. 129, 893–898.

Andrady, A.L., 2011. Microplastics in the marine environment. Mar. Pollut. Bull. 62, 1596–1605.

Andrady, A.L., 2017. The plastic in microplastics: a review. Mar. Pollut. Bull. 119, 12–22.

Barboza, L.G.A., Lopes, C., Oliveira, P., Bessa, F., Otero, V., Henriques, B., Raimundo, J., Caetano, M., Vale, C., Guilhermino, L., 2019. Microplastic in wild fish from North East Atlantic Ocean and its potential for causing neurotoxic effects, lipid oxidative damage, and human health risks associated with ingestion exposure. Sci. Total Environ. 717, 134625.

Bergmann, M., Gutow, L., Klages, M., 2015. Marine Anthropogenic Litter. https://doi.org/10.1007/978-3-319-16510-3.

Burns, E.E., Boxall, A.B.A., 2018. Microplastics in the aquatic environment: evidence for or against adverse impacts and major knowledge gaps. Environ. Toxicol. Chem. 37, 2776–2796.

Carpenter, E.J., Smith Jr., K.L., 1972. Plastics on the sargasso sea surface. Science 175, 1240–1241.

Clukey, K.E., Lepczyk, C.A., Balazs, G.H., Work, T.M., Lynch, J.M., 2017. Investigation of plastic debris ingestion by four species of sea turtles collected as bycatch in pelagic Pacific longline fisheries. Mar. Pollut. Bull. 120, 117–125.

Collins, C., Hermes, J.C., 2019. Modelling the accumulation and transport of floating marine micro-plastics around South Africa. Mar. Pollut. Bull. 139, 46–58.

Deltares, 2011. Delft3D-FLOW User Manual Simulation of Multi-dimensional Hydrodynamic Flows and Transport Phenomena, Including Sediments, User Manual, Hydro Morphodynamics, Version. vol. 3. pp. 15.

Dong, Z., Qiu, Y., Zhang, W., Yang, Z., Wei, L., 2018. Size-dependent transport and retention of micron-sized plastic spheres in natural sand saturated with seawater. Water Res. 143, 518–526.

Ebbesmeyer, C.C., Ingraham, W.J., Jones, J.A., Donohue, M.J., 2012. Marine debris from the Oregon Dungeness crab fishery recovered in the Northwestern Hawaiian Islands: identification and oceanic drift paths. Mar. Pollut. Bull. 65 (1–3), 69–75.

Erdik, T., Şen, O., Öztürk, I., 2019. 3D numerical modeling of exchange flows in Golden Horn Estuary. J. Waterw. Port Coast. Ocean Eng. 145 (5), 04019018.

Filella, M., 2015. Questions of size and numbers in environmental research on microplastics: methodological and conceptual aspects. Environ. Chem. 12 (5), 527–538.

https://doi.org/10.1071/EN15012.
Fischer, H.B., List, J.E., Koh, C.R., Imberger, J., Brooks, N.H., 2013. Mixing in Inland and Coastal Waters. Elsevier.
Geyer, R., Jambeck, J.R., Law, K.L., 2017. Production, use, and fate of all plastics ever made. Science Advance 3, e1700782.
Gregory, M.R., Andrady, A.L., 2003. Plastics in the marine environment. In: Andrady, AnthonyL (Ed.), Plastics and the Environment. John Wiley and Sons (ISBN 0-471-09520-6).
Hahladakis, J.N., Aljabri, H.M.S.J., 2019. Delineating the plastic waste status in the State of Qatar: potentialopportunities, recovery and recycling routes. Sci. Total Environ. 653, 294–299.
Hamza, W., Munawar, M., 2009. Protecting and managing the Arabian Gulf: past, present and future. Aquat. Ecosys. Health Manag. 12, 429–439.
Hardesty, B.D., Harari, J., Isobe, A., Lebreton, L., Maximenko, N., Potemra, J., van Sebille, E., Vethaak, A.D., Wilcox, C., 2017. Using numerical model simulations to improve the understanding of micro-plastic distribution and pathways in the marine environment. Front. Mar. Sci. 4, 30.
Herdman, L., Erikson, L., Barnard, P., 2018. Storm surge propagation and flooding in small tidal rivers during events of mixed coastal and fluvial influence. Journal of Marine Science and Engineering 6 (4), 158.
Hidalgo-Ruz, V., Gutow, L., Thompson, R.C., Thiel, M., 2012. Microplastics in the marine environment: a review of the methods used for identification and quantification. Environmental Science & Technology 46, 3060–3075.
Hinata, H., Sagawa, N., Kataoka, T., Takeoka, H., 2020. Numerical modeling of the beach process of marine plastics: a probabilistic and diagnostic approach with a particle tracking method. Mar. Pollut. Bull. 152, 110910.
Isobe, A., Kubo, K., Tamura, Y., Nakashima, E., Fujii, N., 2014. Selective transport of microplastics and mesoplastics by drifting in coastal waters. Mar. Pollut. Bull. 89, 324–330.
Jambeck, J.R., Geyer, R., Wilcox, C., Siegler, T.R., Perryman, M., Andrady, A., Narayan, R., Law, K.L., 2015. Plastic waste inputs from land into the ocean. Science 347, 768–771.
Kaiser, D., Kowalski, N., Waniek, J., 2017. Effects of biofouling on the sinking behavior of microplastics. Environ. Res. Lett. 12 (12).
Kako, S.I., Isobe, A., Seino, S., Kojima, A., 2010. Inverse estimation of drifting-object outflows using actual observation data. J. Oceanogr. 66 (2), 291–297.
Kämpf, J., Sadrinasab, M., 2006. The circulation of the Persian Gulf: a numerical study. Ocean Sci. 2, 27–41.
Kor, K., Mehdinia, A., 2020. Neustonic microplastic pollution in the Persian Gulf. Mar. Pollut. Bull. 150, 110665.
Law, K.L., Moret-Ferguson, S., Maximenko, N.A., Proskurowski, G., Peacock, E.E., Hafner, J., 2010. Plastic accumulation in the North Atlantic subtropical gyre. Science 329 (5996), 1185–1188.
Lyons, B.P., Cowie, W.J., Maes, T., Le Quesne, W.J.F., 2020. Marine plastic litter in the ROPME Sea Area: current knowledge and recommendations. Ecotoxicol. Environ. Saf. 187, 109839.
Mahdavimanesh, M., Noghrehabadi, A.R., Behbahaninejad, M., Ahmadi, G., Dehghanian, M., 2013. Lagrangian particle tracking: model development. Life Science Journal 10, 34–41.
Martin, C., Agustí, S., Duarte, C.M., 2019. Seasonality of marine plastic abundance in central Red Sea pelagic waters. Sci. Total Environ. 688, 536–541.
Maximenko, N., MacFadyen, A., Kamachi, M., 2015. Modeling the drift of marine debris generated by the 2011 tsunami in Japan. PICES Press 23 (2), 32–36.
Morét-Ferguson, S., Law, K.L., Proskurowski, G., Murphy, E.K., Peacock, E.E., Reddy, C.M., 2010. The size, mass, and composition of plastic debris in the western North Atlantic Ocean. Mar. Pollut. Bull. 60, 1873–1878.
Muthukumar, T., Aravinthan, A., Lakshmi, K., Venkatesan, R., Vedaprakash, L., Doble, M., 2011. Fouling and stability of polymers and composites in marine environmentInt. Biodeter. Biodegrad. 65 (2), 276–284.
Naji, A., Esmaili, Z., Khan, F.R., 2017a. Plastic debris and microplastics along the beaches of the Strait of Hormuz, Persian Gulf. Mar. Pollut. Bull. 114, 1057–1062.
Naji, A., Esmaili, Z., Mason, S.A., Vethaak, A.D., 2017b. The occurrence of microplastic contamination in littoral sediments of the Persian Gulf, Iran. Environ. Sci. Pollut. Res. 24, 20459–20468.
Naji, A., Nuri, M., Vethaak, A.D., 2018. Microplastics contamination in molluscs from the northern part of the Persian Gulf. Environ. Pollut. 235, 113–120.
Naji, A., Nuri, M., Amiri, P., Niyogi, S., 2019. Small microplastic particles (S-MPPs) in sediments of mangrove ecosystem on the northern coast of the Persian Gulf. Mar. Pollut. Bull. 146, 305–311.
Núñez, P., García, A., Mazarrasa, I., Juanes, J.A., Abascal, A.J., Méndez, F., Castanedo, S., Medina, R., 2019. A methodology to assess the probability of marine litter accumulation in estuaries. Mar. Pollut. Bull. 144, 309–324.
Okubo, A., 1971. Oceanic diffusion diagrams. In: Deep Sea Research and Oceanographic Abstracts. vol. 18. Elsevier, pp. 789–802 (8).
Oliveira, M., Almeida, M., 2019. The why and how of micro(nano)plastic research. Trends Anal. Chem. 114, 196–201.
Oliveira, V.H., Sousa, M.C., Morgado, F., Dias, J.M., 2019. Modeling the impact of extreme river discharge on the nutrient dynamics and dissolved oxygen in two adjacent estuaries (Portugal). Journal of Marine Science and Engineering 7 (11), 412.
Ouyang, W., Zhang, Y., Wang, L., Barceló, D., Wang, Y., Lina, C., 2020. Seasonal relevance of agricultural diffuse pollutant with microplastic in the bay. J. Hazard. Mater. 396, 122602.
Palatinus, A., Viršek, M.K., Robič, U., Grego, M., Bajt, O., Šiljić, J., Suaria, G., Liubartseva, S., Coppini, G., Peterlin, M., 2019. Marine litter in the Croatian part of the middle Adriatic Sea: simultaneous assessment of floating and seabed macro and micro litter abundance and composition. Mar. Pollut. Bull. 139, 427–439.
Pokavanich, T., Alosairi, Y., 2014. Summer flushing characteristics of Kuwait Bay. J. Coast. Res. 30, 1066–1073.
Politikos, D.V., Tsiaras, K., Papatheodorou, G., Anastasopoulou, A., 2020. Modeling of floating marine litter originated from the Eastern Ionian Sea: transport, residence time and connectivity. Mar. Pollut. Bull. 150, 110727.
Pous, S., Carton, X., Lazure, P., 2012. A process study of the tidal circulation in the Persian Gulf. Open Journal of Marine Science 2, 131.
Pous, S., Carton, X., Lazure, P., 2013a. A process study of the wind-induced circulation in the Persian Gulf. Open Journal of Marine Science 3, 11.
Pous, S., Carton, X., Lazure, P., 2013b. A process study of the wind-induced circulation in the Persian Gulf. Open J. Mar. Sci 3, 27160.
Rangel-Buitrago, N., Gracia, A., Velez-Mendoza, A., Carvajal-Florián, A., Mojica-Martinez, L., Neal, W.J., 2019. Where did this refuse come from? Marine anthropogenic litter on a remote island of the Colombian Caribbean Sea. Mar. Pollut. Bull. 149, 110611.
Reisser, J., Shaw, J., Wilcox, C., Hardesty, B.D., Proietti, M., Thums, M., Pattiaratchi, C., 2013. Marine plastic pollution in waters around Australia: characteristics, concentrations, and pathways. PLoS One 8 (11), e80466.
Rubinstein, R., 1981. Simulation and the Monte Carlo Method. Wiley, New York.
Ryan, P.G., 2015. A brief history of marine litter research. In: Marine Anthropogenic Litter. Springer, Cham, pp. 1–25.
Stuparu, D., Van Der Meulen, M., Kleissen, F., Vethaak, D., El Serafy, G., 2015. Developing a transport model for plastic distribution in the North Sea. In: E-proceedings of the 36th IAHR World Congress 28 June - 3 July, 2015, The Hague, The Netherlands.
Tang, Y., Rong, J., Guan, X., Zha, S., Shia, W., Han, Y., Du, X., Wu, F., Huang, W., Liu, G., 2020. Immunotoxicity of microplastics and two persistent organic pollutants alone or in combination to a bivalve species. Environ. Pollut. 258, 113845.
Thompson, R.C., Olsen, Y., Mitchell, R.P., Davis, A., Rowland, S.J., John, A.W.G., McGonigle, D., Russel, A.E., 2004. Lost at sea: where is all the plastic? Science 304, 838.
Thoppil, P.G., Hogan, P.J., 2010. A modeling study of circulation and eddies in the Persian Gulf. J. Phys. Oceanogr. 40, 2122–2134.
van der Hal, N., Ariel, A., Angel, D.L., 2017. Exceptionally high abundances of microplastics in the oligotrophic Israeli Mediterranean coastal waters. Mar. Pollut. Bull. 116, 151–155.
van Utenhove, E.J.F., 2019. Modelling the Transport and Fate of Buoyant Macroplastics in Coastal Waters. Master of Science thesis. Delft University of Technology, Delft, The Netherlands.
Wagner, M., Scherer, C., Alvarez-Munor, D., Brennholt, N., Bourrain, X., Buchinger, S., Fries, E., Grosbois, C., Klasmeier, J., Marti, T., Rodriguez-Mozaz, S., Urbatzka, R., Vethaak, A.D., Winther Nielsen, M., Reifferscheid, G., 2014. Microplastics in freshwater ecosystems: what we now and what we need to know. Environ. Sci. Eur. 26, 12–20.
Westall, S., Hagagy, A., 2019. Kuwait Plan for Northern Mega City Faces Political Hurdles. Business News, Reuters.
Zhang, H., 2017. Transport of microplastics in coastal seas. Estuar. Coast. Shelf Sci. 199, 74–86.